Engineered Science

RESEARCH PAPER

View Article Online

Tunable Thermal-Response Shape Memory Bio-Polymer Hydrogelsas Body Motion Sensors

Hailong Huang,[#] Lu Han,[#] Yangling Wang, Zhongli Yang, Feng Zhu and Min Xu[*]

Wearable health monitoring smart systems are considered to be the next generation artificial intelligence devices for real-time tracking down human body motion. However, due to the stress relaxation and viscosity, the existed stretching sensor, especially most ultra-stretching ones, are hard to recover to their original shape after cycles repeatedly stretching, leading to inspection hysteresis and shorter service life. Herein, we reported an intelligent ionic conductive hydrogel (SAMA) as stretching sensor with good mechanical property and controllable thermal-response shape memory property. The obtained hydrogel sensor exhibited outstanding sensitivity to human body motion. Besides, it had a controllable upper critical solution temperature (UCST) from 15 ºC to 58 ºC through adjusting the concentration of Li^+ in the hydrogel. When temperature above UCST, the deformed hydrogel could quickly recover to original shape within 30 seconds and regain sensitive inspection ability. Moreover, the shape memory ability of SAMA hydrogel exhibited a good reuseability at least 50 cycles. The unique stretching hydrogel sensor with controllable thermal-response shape memory could effectively solve the deformation problem of stretching sensor and prolong the service life, demonstrating great potential in the flexible wearable electronics and biologic devices.

Keywords: Stretchable sensor; Ionic conductive hydrogel; Body motion detection; Shape memory; Thermal response

Received 25 February 2019, **Accepted** 3 April 2019

DOI: 10.30919/es8d812

1. Introduction

During the past decade, flexible electronic devices have earned great achievements and attracted much interests,[1-7] especially the stretching sensor which has been greatly developed in wearable electronics devices,[8-14] flexible luminescence devices[15-18] and soft robotics.[19-25] Among different kinds of stretching sensor, ionic conductive hydrogel stretching sensor is considered to be the best materials for the human body motion sensor, due to the good electrochemical performance[26-34] and controllable mechanical properties.[35-37] Many studies have been focused on the hydrogel stretching sensors. Alshareef [38] reported a MXene-based hydrogel (M-hydrogel) exhibited good sensitivity for detecting body motions with excellent elongation of nearly 3400 %. Sui[39] mimicked dermis structures to prepared a double network ionic hydrogel with natural polymer sodium alginate nanofibrillar, which shown good flexibility to a broad strain window for the sports monitoring. Wu[40] fabricated multiple sensations ionic hydrogel sensor with good sensations towards strain, stress, touch, humidity and temperature. Under the remote control of a NIR laser, the polyionic sensor could gradually transform from bending to stretching and showed good repeatability.

However, there exists a serious shortage limiting the development of stretching sensor as wearable electronic detection, which is the stress relaxation. At present, there are two types of stretching sensors for the human body motion. One is ultra-stretching sensor with low tensile stress and high tensile strain. It cannot recover to the original shape after overstretching. The other is flexible stretching sensor with high tensile stress and low tensile strain. It can recover to original shape only in small strain. Attributed to these problems, the existed stretching hydrogel sensors cannot satisfy the needs of ideal stretching sensor for the human

School of Physics and Materials Science & Shanghai Key Laboratory of Magnetic Resonance, East China Normal University, No. 3663 North Zhongshan Road, Shanghai 200062, China

[#]Author Contributions: Hailong Huang and Lu Han contributed equally

***E-mail:** xumin@phy.ecnu.edu.cn (M. Xu)*

© Engineered Science Publisher LLC 2020

body motion detection. Importantly, the unrecoverable deformation of stretching hydrogel sensor could not make the hydrogel sensor tightly stick on the human body, and then, resulting in response hysteresis and service life degradation. Although lots of researchers work in stretching hydrogel sensor, few work pay attention to solve stress relaxation for the stretchable sensor.

In this work, we designed a series of stretching hydrogel (SAMA) with excellent mechanical property and shape memory ability. Functional monomer and metal ion were introduced into sodium alginate framework to fabricate a double network conductive hydrogel. Due to the goog flexibility and conductivity, the SAMA hydrogel sensor exhibited excellent sensitivity to inspect body motion with different strength, frequency and gesture synchronously. Besides, based on the thermal-response shape memory performance, the hydrogel sensor revealed excellent shape recovery ability. It could easily escape from the unrecoverable deformation and quickly recover to the original shape through thermal-response ability. More importantly, the recovered stretching hydrogel sensor maintained good flexibility and sensitivity with good reuseability. Hence, the SAMA exhibited greatly potential applications in wearable electronics devices with sensitive detection and reversible shape recovery properties.

2. Experiment Section

2.1 Materials

Sodium alginate was obtained from Aladdin Chemical Co. Acrylic acid (AA), acrylamide (AM), sodium chloride (LiCl), ammonium persulfate (APS) were purchased from Aladdin Chemical Co and used as received.

2.2 Preparation of SA/P(AA-AM)/LiCl Hydrogels (SAMA)

The SAMA shape memory hydrogels were prepared by free radical polymerization. 1.0 g AM, 2.0 g AA and 5.0 g water were put into 4.5 g SA aqueous solution under stirring at room temperature, until the monomer of AM and AA completely dissolved. Then 0.1 g LiCl and 6 % (wt) APS were added into the mixture and kept stirring for 10 mins. After that, the reaction was carried out at 55 °C for 8 h. The different concentration of LiCl in SAMA hydrogels were prepared as shown in Table 1.

2.3 Characterization

The chemical structure was measured by Fourier transform infrared spectroscopy (FTIR) spectra on Nicolet-Nexus 670 spectrophotometer at room temperature. XRD data were recorded using X-ray diffractometer (Holland Panalytical PRO PW 3040/60, V = 35 kV, I = 25 mA, $\lambda = 1.5418$ Å), in the 2θ range 10-80 °, at a scanning rate of 10 ° min^{-1}. The concentration of Li^+ in the SAMA was measured by ICP[41] (Varian 720-ES). The microtopography of SAMA hdyrogel was tested using Hitachi S-4800 filed emission scanning electron microspoce. The mechanical property of SAMA hydrogel was measured on Instron 5967 tensile machine. The stress-strain speeds for the compression and stretching were 2 mm/min and 20 mm/min at 25 °C, respectively. The thermal response ability was studied by turbidimetry with UV-Vis spectrometer (from 5 °C to 65 °C). The temperature at 50 % transmittance of thermal transition was taken as the UCST.

2.4 Body Motion Detection

In order to study the performance of SAMA hydrogel sensor,. the SAMA hydrogel were connected with PARSTAT4000A via copper wires to record the relative resistance changes. To monitor the subtle movement, a SAMA-3 hydrogel frame (length × width × thickness is 60 mm × 10 mm × 1 mm) was fabricated and adhered to the index finger. For the detecting human body motion, the same SAMA-3 hydrogel frame was adhered to the elbow and knee. The conductive tape was used to protect the electrodes to prevent unstable contact and electrode motion.

2.5 Shape Memory Property

The helical shaped SAMA hydrogel was prepared to study the deformation and resistance changes during the shape memory process. An as-prepared helical SAMA-3 hydrogel with length of 4.35 cm was stretched repeatedly more than 30 times until unrecoverable deformation occurred. Then, the deformed SAMA-3 hydrogel was put into hot water of 65 °C and the deformation process was recorded. After the SAMA-3 hydrogel recovered to its original shape, and then cooled to 25 °C. The changes of the relative resistance and length were recorded by

Table 1 Contents of SAMA hydrogels.

	SA (g)	AM (g)	AA (g)	H_20 (g)	LiCl (g)
SAMA-0	4.5	1.0	2.0	5.0	0
SAMA-1	4.5	1.0	2.0	5.0	0.1
SAMA-2	4.5	1.0	2.0	5.0	0.3
SAMA-3	4.5	1.0	2.0	5.0	0.5

© Engineered Science Publisher LLC 2020

continuous 50 helical-stretch-helical cycles.

3. Results and discussion

For the stretching sensor, the unrecoverable deformation always is a serious problem due to the viscoelasticity and stress relaxation, resulting in detection inefficiency and service life degradation. Although many efforts are performed were developed, such as improving the mechanical property, introducing self-healing ability and so on, the unrecoverable deformation for the stretching sensor is not effectively solved. In order to solve the deformation, we fabricated an ionic conductive hydrogel (SAMA) with thermal-response shape memory property. Based on the framework of SA, functional monomers and metal ion were introduced to build a double network structure conductive hydrogel. The microstructure of SAMA hydrogel is shown in Fig. 1A.

The chemical structure of SAMA hydrogels were confirmed by IR, SEM and ICP as shown in Figs. 1(B-D). The characteristic peaks of AA attribute to -OH stretching at 3430 cm^{-1}, -C=O stretching at 1680 cm^{-1} and -C=C stretching at 1630 cm^{-1}. The characteristic peaks of AM locate at 3400 cm^{-1}, 3300 cm^{-1} and 1620 cm^{-1}, which are related to the stretching vibrations of $-NH_2$, -C=C and -C=O, respectively. The characteristic peaks of SA correspond to -OH stretching at 3540 cm^{-1}, $-CH_3$ stretching at 2980 cm^{-1}, -C=O stretching at 1620cm^{-1} and -C-O-C- stretching at 1250 cm^{-1}. In the FTIR spectrum of SAMA hydrogel, all characteristic peaks of AA, AM and SA were observed, indicating that the SAMA hydrogel was successfully synthesized. The appeared characteristic peaks on the XRD pattern of SAMA can be indexed to LiCl (JCPDS, File No. 05-0628) and the amorphous nature of SAMA hydrogel is confirmed by the broad peaks centered at 18° and 32°.

From Figs. 1(D-G), the porous framework can be observed clearly in the SAMA-0, and plenty of LiCl particles were observed at the surface of SAMA(1-3), which is attributed to the precipitated LiCl during freeze drying. The concentration of Li^+ was measured by ICP as shown in Table 2. The concentration of Li^+ ion was 0.62 % for SAMA-1, 1.11 % for SAMA-2 and 2.08 % for SAMA-3, respectively.

Through the stress-strain measurements, all the SAMA hydrogels exhibits good mechanical properties as shown in Figs. 1(H-G) and Table 2. The mechanical properties of SAMA showed remarkable improvement with increase concentration of Li^+ from 0.62 % to 2.08 %. The tensile strength increased from 0.17 Mpa to 0.38 Mpa and compress strength increased from 0.23 Mpa to 0.34 Mpa. Among the three SAMA(1-3) hydrogels, SAMA-3 revealed the best stress strength, tensile strength and stain. It was attributed to dynamic interaction between Li^+ and carboxylate. The increase concentration of Li^+ could

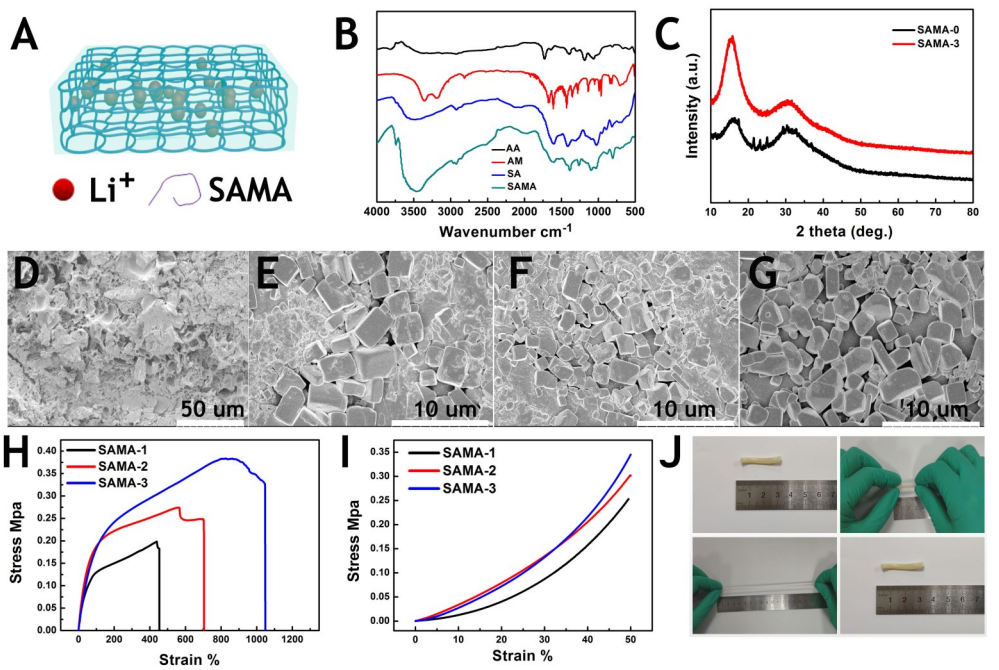

Fig. 1 (A) Schematic structure of SAMA hydrogel. (B) FTIR spectra of AA, AM, SA and SAMA. (C) XRD pattern of SAMA-0 and SAMA-3. The SEM images of hydrogels: (D) SAMA-0, (E) SAMA-1, (F) SAMA-2, (G) SAM-3. Mechanical properties of SAMA hydrogels: (H) Tensile stress – strain curves and (I) Compress stress – strain curves (J) Demonstration of the flexible SAMA-3 hydrogel.

© Engineered Science Publisher LLC 2020

effectively increase the cross-link degree to improve the mechanical property. [42] Thus, through adjusting the Li^+ concentration, the SAMA hydrogel with different mechanical strength could be prepared to satisfy the requirements of different applications.

3.1 Body Motion Sensor

Due to the good flexibility and sensitivity, when the hydrogel is stretched, the deformation of hydrogel can induce its resistance changes. Through the mechanotransduction signals, the stretching hydrogel sensor can translate the deformation caused by body movement into visual electrical signals to reflect the human body motion. As shown in Figs. 2(A-B), the SAMA-3 was attached to the index finger to detect the finger motion. It could be found that the SAMA-3 exhibited sensitive detection during the finger bending-stretching process. For the different bending angles from 0° to 90°(a: 0°, b: 30°, c: 60°, d: 90°), the SAMA-3 could make accurate feedback via the resistance changes from 20 % to 60 % to respond finger bending angles in real time. Besides, during the continuously bending process, the bending angles and times also could be easily distinguished through the signal strength and the number of signal peaks. In order to demonstrate the timeliness of SAMA-3, the slow bending process at different time intervals were measured, as shown in Fig. 2C. The

Table 2 Mechanical properties of SAMA hydrogels.

	Li (wt%)	tensile strength (Mpa)	elongation at break (%)	modulus of elasticity (Mpa)	compressive strength (Mpa)	modulus of compression (Mpa)
SAMA-1	0.62%	0.17	456.27	0.24	0.23	0.06
SAMA-2	1.11%	0.26	697.94	0.38	0.32	0.27
SAMA-3	2.08%	0.38	1080.88	0.53	0.34	0.33

Table 3 The equivalent series resistance of SAMA hydrogels at different temperature.

	UCST(°C)	RΩ (10 °C)	RΩ (65 °C)
SAMA-1	15	60.4	22.1
SAMA-2	33	84.8	12.6
SAMA-3	58	103.8	10.1

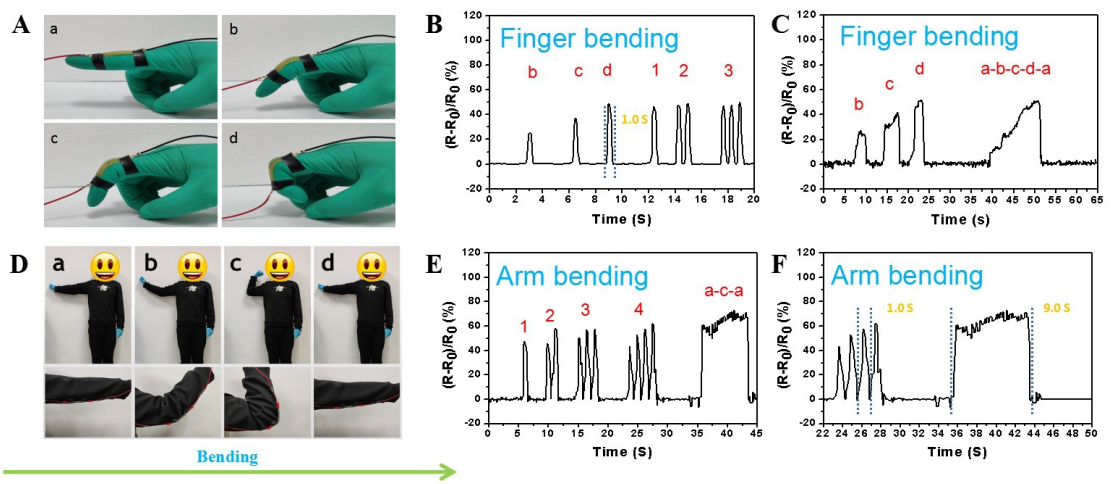

Fig. 2 (A) Schematic of SAMA-3 hydrogel mounted on the finger for monitoring the finger motion state (a: 0°, b: 30°, c: 60°, d: 90°). (B-C) Resistance changes of the stretching sensor during continuously index finger bending and releasing processes. (D) Schematic of SAMA-3 hydrogel mounted on the elbow for monitoring the arm motion. (E-F) Resistance changes of the stretching sensor during continuously arm bending and releasing processes.

© Engineered Science Publisher LLC 2020

SAMA-3 hydrogel sensor revealed excellent sensitivity and timeliness. More importantly, SAMA-3 exhibited good sensitivity up to 2 Hz, as shown in Fig. S1. In order to investigate the reusability, the stability of SAMA-3 was measured. As shown in Fig. S2, the SAMA-3 maintained stable resistance changes during the stability test at tensile strain of 20% for 350 loading/unloading cycles, suggesting good stability of SAMA-3.

To further investigate the performance of the stretching hydrogel sensor, SAMA-3 was attached to elbow to detect the body motion again. For the arm motion, the SAMA-3 showed good detection ability. It could be observed from Figs. 2(D-F) that the electronic signals were clear and stable during the repeated bending-stretching process, and the number of signal peaks were consistent with the arm bending times sensitively from 1 to 4 times without hysteresis. More important, when changing the motion time of bending-stretching process (a-c-a) from 1.0 s to 9.0 s, the SAMA-3 also maintained excellent sensitivity and timeliness to reflect the arm bending process.

Besides finger and elbow motion detection, we also detected the leg movement by monitoring the knees motion. As shown in Figs. 3(A-H), during the continuous leg motion processes with different times and frequency, the movements were clearly identified by the resistance change of times and bending angles in real time. Interestingly, compared with finger and elbows motion, the electronic

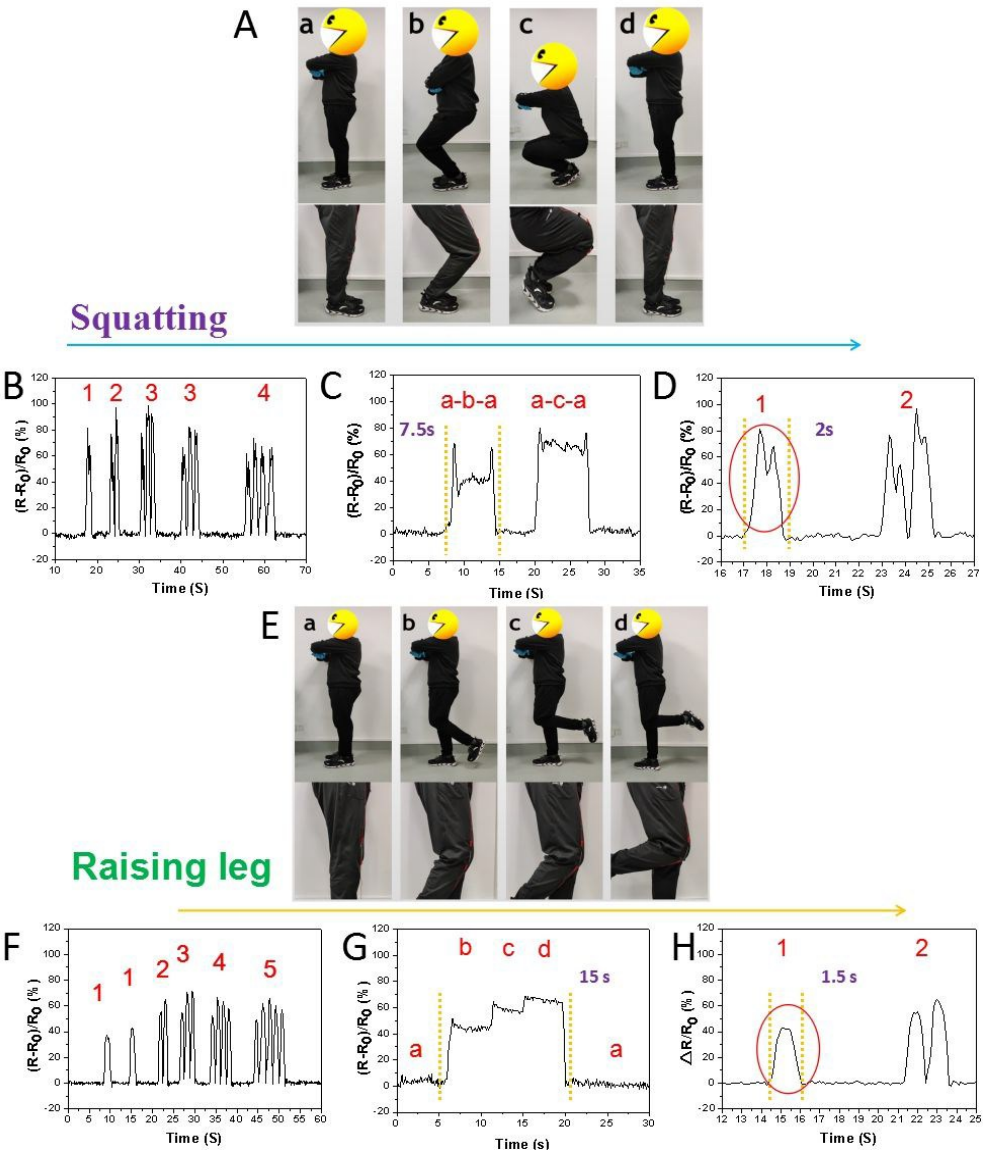

Fig. 3 (A) Schematic of SAMA-3 hydrogel mounted on the knee for monitoring the leg motion state. (B-D) Resistance changes of the stretching sensor during continuously squatting and rising processes. (E) Schematic of SAMA-3 hydrogel mounted on the knee for monitoring the leg motion. (F-H) Resistance changes of the stretching sensor during continuously leg bending and releasing processes.

© Engineered Science Publisher LLC 2020

signals exhibited different characteristic peaks between squatting and raising leg motions. Compared with single peak of raising leg process, there was an obvious split peaks of squatting process. Thus, it could be easily to distinguish the leg movement gesture according to the significant difference of leg motion signals, Hence, the stretching SAMA-3 hydrogel sensor not only exhibited sensitively and synchronously human body motion detection for the motion strength and frequency, but also possessed good identification for motion gesture detection between squatting and raising leg.

3.2 Shape Memory Performance

However, due to the stress relaxation, the hydrogel cannot recover to the original shape from deformation induced cycles for repeatedly stretching, leading to response insensitivity with hysteresis and service life degradation. While fortunately, besides the good human body motion detection performance, the SAMA also had good thermal-response shape memory property. As shown in Fig. 4A, the thermal response ability of SAMA hydrogels were measured at 700 nm with different temperature from 5 °C to 65 °C. It is observed that all the SAMA hydrogels exhibits typical behavior of upper critical solution temperature (UCST). When the temperature increased above the UCST, the SAMA hydrogels changed from ivory-white opaque to yellowish transparent and maintained stable. When the temperature reduced to room temperature, the transparent hydrogels recovered to opaque state again, suggesting the SAMA hydrogels possessed a sensitive and reversible UCST. Importantly, it is noting that the transition temperature can be adjusted from 15 °C to 58 °C by changing the concentration of Li^+ in SAMA hydrogels (15 °C SAMA-1, 33 °C SAMA-2 and 58 °C SAMA-3).

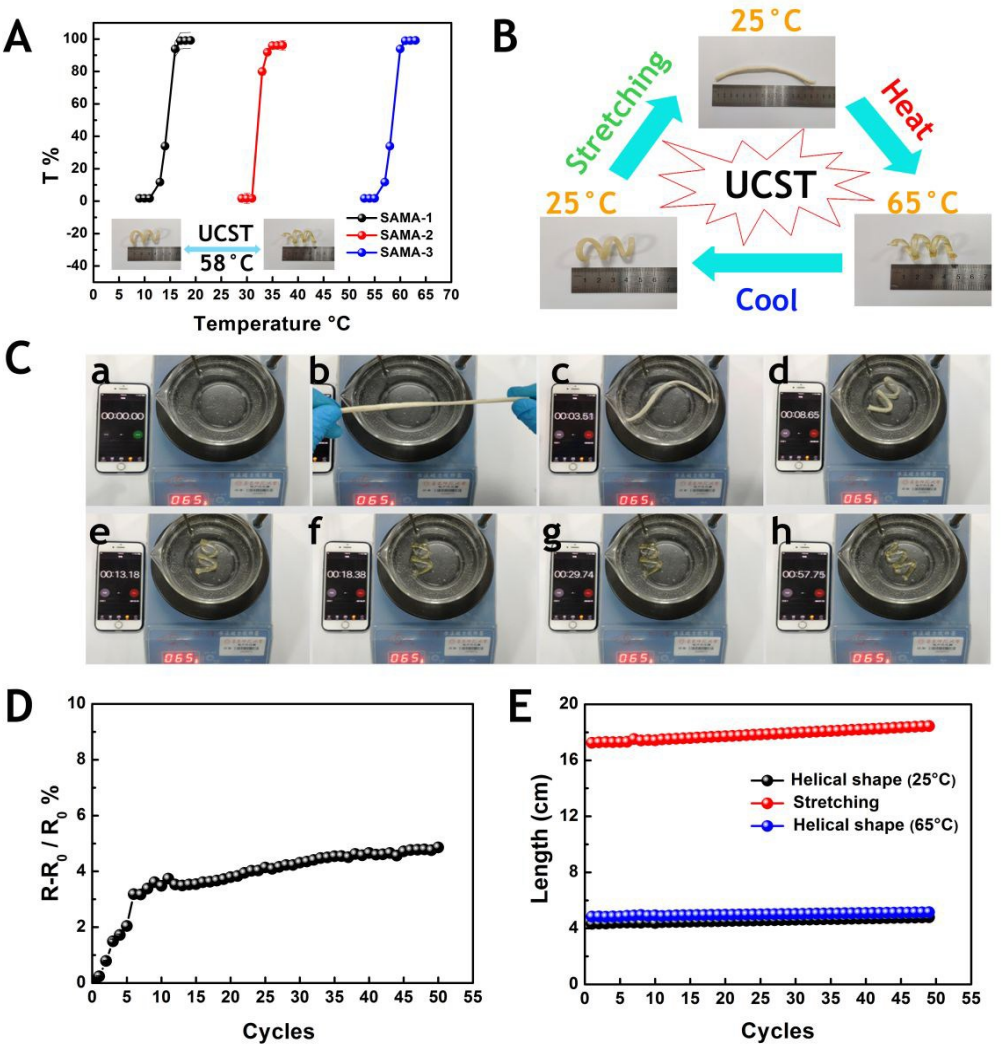

Fig. 4 (A) Temperature response properties of hydrogels SMA-1, SAM-2 and SAM-3, respectively. Insert: the helical shape SAMA-3 temperature response. (B) The shape memory performance of SAMA-3 hydrogel helical-line-helical process. (C) The time-dependent relative shape changes at 65 °C. The recyclability of SAMA-3 hydrogels after 50 shape memory cycles: (D) Resistance changes and (E) Length changes.

© Engineered Science Publisher LLC 2020

We used the thermal responsiveness as trigger to control the shape memory process of SAMA-3. In order to investigate the shape memory property, the helical shape hydrogel was prepared as shown in Fig. 4B. We simulated the stress relaxation of stretching sensor through multiple tension-relaxation cycles, until it could not recover to its original shape. Then, put the deformed hydrogel into hot water 65 °C above the UCST to observe the shape recovery process as shown in Figs. 4(B-C) and video SI-1. It could be found the deformed SAMA-3 quickly changed from ivory-white and opaque hydrogel to yellowish and transparent one obviously, and while twisted back into a helical shape without any external force. Then, when the SAMA-3 cooled to the room temperature, it returned back to ivory-white and opaque one again. And the helical shape and length also recovered again without hysteresis. More importantly, the shape recovery process only needed 30 seconds and no rebound was observed, which is much better than most reported recoverable hydrogel sensor (Table S1). Besides, the reuseability of SAMA-3 hydrogel was investigated through the changes of resistance and length in 50 deform-recover cycles.[43] To avoid the loss of water and salt, LiCl solution(the same concentration with hydrogel) was used at recovery process. From Fig. 4D, during the first 7 recovery cycles, obvious changes of resistance was observed, but below 4%. After that, the resistance of SAMA-3 maintained good stability and the overall changes was below 5 %. Meanwhile, the length of SAMA-3 hydrogel also exhibited good stability during shape recovery cycles and the changes was below 3 %. These outstanding performance indicated that SAMA-3 hydrogel sensor not only exhibited good detection and identification ability for the human body motions, but also reveals outstanding shape recovery property to solve the problem of stress relaxation and prolong the service life.

4. Conclusion

In this paper, we developed a novel thermal-response shape memory natural polymer based hydrogel SAMA as human body motion sensor. The SAMA hydrogel exhibited good mechanical property, controllable thermal responsiveness and excellent sensitivity to detect the human body motions involving in bending finger, bending arms, raising leg and squatting. More important, the unique thermal-response shape memory property of SAMA hydrogel sensor effectively solve the problem of unrecoverable deformation for the stretching sensor, which provided a convenient method to prolong the life of stretching sensor, demonstrating a great potential for human body motion detection.

Acknowledgments

This work is sponsored by the National Natural Science Foundation of China (No. 21875068).

References

1. H. Fang, K. J. Yu, C. Gloschat, Z. Yang, C. Chiang, J. Zhao, S. M. Won, S. Xu, M. Trumpis, Y. Zhong, E. Song, S. W. Han, Y. Xue, D. Xu, G. Cauwenberghs, M. Kay, Y. Huang, J. Viventi, I. R. Efimov and J. A. Rogers, *Nat. Biomed. Eng.*, 2017, **1**, 38.
2. C. G. Núñez, W. T. Navaraj, E. O. Polat and R. Dahiya, *Adv. Funct. Mater.*, 2017, **27**, 1606287.
3. Y. Li, L. Meng, Y. M. Yang, G. Xu, Z. Hong, Q. Chen, J. You, G. Li, Y. Yang and Y. Li, *Nat. Commun.*, 2016, **7**, 10214.
4. F. R. Fan, W. Tang and Z. L. Wang, *Adv. Mater.*, 2016, **28**, 4283-4305.
5. A. J. Baca, J. Ahn, Y. Sun, M. A. Meitl, E. Menard, H. Kim, W. M. Choi, D. Kim, Y. Huang and J. A. Rogers, *Angew. Chem. Int. Ed*, 2008, **47**, 5524-5542.
6. Z. Lei and P. Wu, *ACS Nano*, 2018, **12**, 12860-12868.
7. Y. Li, G. Zhu, H. Huang, M. Xu, T. Lu and L. Pan, *J. Mater. Chem. A*, 2019, **7**, 9040-9050.
8. W. Zeng, L. Shu, Q. Li, S. Chen, F. Wang and X. Tao, *Adv. Mater.*, 2014, **26**, 5310-5336.
9. J. Ren, W. Bai, G. Guan, Y. Zhang and H. Peng, *Adv. Mater.*, 2013, **25**, 5965-5970.
10. M. Ha, J. Park, Y. Lee and H. Ko, *ACS Nano*, 2015, **9**, 3421-3427.
11. Y. Gao, Q. Li, R. Wu, J. Sha, Y. Lu and F. Xuan, *Adv. Funct. Mater.*, 2019, **29**, 1806786.
12. X. Fang, J. Tan, Y. Gao, Y. Lu and F. Xuan, *Nanoscale*, 2017, **9**, 17948.
13. Q. Li, J. Li, D. Tran, C. Luo, Y. Gao, C. Yu and F. Xuan, *J. Mater. Chem. C*, 2017, **5**, 11092.
14. J. Zhang, L. Wan, Y. Gao, X. Fang, T. Lu, L. Pan and F. Xuan, *Adv. Electron. Mater.*, 2019, **5**, 1900285.
15. X. Qian, Z. Cai, M. Su, F. Li, W. Fang, Y. Li, X. Zhou, Q. Li, X. Feng, W. Li, X. Hu, X. Wang, C. Pan and Y. Song, *Adv. Mater.*, 2018, **30**, 1800291.
16. Y. Zhuang, L. Wang, Y. Lv, T. Zhou and R. Xie, *Adv. Funct. Mater.*, 2018, **28**, 1705769.
17. T. Li, J. Zou, F. Xing, M. Zhang, X. Cao, N. Wang and Z. L. Wang, *ACS Nano*, 2017, **11**, 3950-3956.
18. Y. Liu, Z. Liu, B. Zhu, J. Yu, K. He, W. R. Leow, M. Wang, B. K. Chandran, D. Qi, H. Wang, G. Chen, C. Xu and X. Chen, *Adv. Mater.*, 2017, **29**, 1701780.
19. J. Z. Gul, M. Sajid, M. M. Rehman, G. U. Siddiqui, I. Shah, K. Kim, J. Lee and K. H. Choi, *Sci. Technol. Adv. Mat.*, 2018, 243-262.
20. J. K. Wassei and R. B. Kaner, *Mater. Today*, 2010, **13**, 52-59.
21. R. Ramachandramoorthy, Y. Wang, A. Aghaei, G. Richter, W. Cai and H. D. Espinosa, *ACS Nano*, 2017, **11**, 4768-4776.
22. J. Wang, M. Liang, Y. Fang, T. Qiu, J. Zhang and L. Zhi, *Adv. Mater.*, 2012, **24**, 2874-2878.
23. P. Lorwongtragool, E. Sowade, N. Watthanawisuth, R. R. Baumann and T. Kerdcharoen, *Sensors*, 2014, **14**, 19700-19712.
24. T. Q. Trung and N. Lee, *Adv. Mater.*, 2016, **28**, 4338-4372.
25. Y. Lo, W. Lee and C. Liu, *J. Med. Syst*., 2013, **37**, 9923.
26. Z. Lei, Q. Wang, S. Sun, W. Zhu and P. Wu, *Adv. Mater.*, 2017, **29**, 1700321.
27. A. V. Thakur and B. J. Lokhande, *J. Mater. Sci: Mater. Electron.*, 2017, **28**, 11755-11761.
28. R. K. Pal, S. C. Kundu and V. K. Yadavalli, *ACS Appl. Mater. Inter.*, 2018, **10**, 9620-9628.
29. M. Mao, C. Cui, M. Wu, M. Zhang, T. Gao, X. Fan, J. Chen, T. Wang, J. Ma and C. Wang, *Nano Energy*, 2018, **45**, 346-352.
30. A. Kumar, M. L. Singla, A. Kumar and J. K. Rajput, *J. Mater. Sci: Mater. Electron.*, 2015, **26**, 1838-1852.
31. X. Peng, H. Liu, Q. Yin, J. Wu, P. Chen, G. Zhang, G. Liu, C. Wu and Y. Xie, *Nat. Commun.*, 2016, **7**, 11782.
32. J. Chupp, A. Shellikeri, G. Palui and J. Chatterjee, *J. Appl. Polym. Sci.*, 2015, **132**, 42143.

 © Engineered Science Publisher LLC 2020

33. C. Yang and Z. Suo, *Nat. Rev. Mater.*, 2018, **3**, 125-142.
34. C. Keplinger, J. Sun, C. C. Foo, P. Rothemund, G. M. Whitesides and Z. Suo, *Science*, 2013, **341**, 984-987.
35. Q. Chen, X. Yan, L. Zhu, H. Chen, B. Jiang, D. Wei, L. Huang, J. Yang, B. Liu and J. Zheng, *Chem. Mater.*, 2016, **28**, 5710-5720.
36. J. Wang, J. Wei, S. Su, J. Qiu and S. Wang, *J. Mater. Sci.*, 2015, **50**, 5458-5465.
37. X. Li, C. Wu, Q. Yang, S. Long and C. Wu, *Soft. Matter.*, 2015, **11**, 3022-3033.
38. Y. Zhang, K. H. Lee, D. H. Anjum, R. Sougrat, Q. Jiang, H. Kim and H. N. Alshareef, *Sci. Adv.*, 2018, **4**, eaat0098.
39. X. Zhang, N. Sheng, L. Wang, Y. Tan, C. Liu, Y. Xia, Z. Nie and K. Sui, *Mater. Horiz.*, 2019, **6**, 326-333.
40. Z. Lei and P. Wu, *Mater. Horiz.*, 2019, **6**, 538-545
41. M. Kawalec, A. P. Dove, L. Mespouille and P. Dubois, *Polym. Chem.*, 2013, **4**, 1260-1270.
42. F. Shi, M. Zhong, L. Zhang, X. Liu and X. Xie, *Chinese J. Polym. Sci.*, 2017, **35**, 25-35
43. Y. Zhang, J. Liao, T. Wang, W. Sun and Z. Tong, *Adv. Funct. Mater.*, 2018, **28**, 1707245.

Publisher's Note Engineered Science Publisher remains neutral with regard to jurisdictional claims in published maps and institutional affiliations.

© Engineered Science Publisher LLC 2020